In a Collaborative Co-manipulation, Humans Have a Motor Behaviour Similar to a Leader

Waldez Gomes, Pauline Maurice, Jan Babič, Jean-Baptiste Mouret, Serena Ivaldi

In a Collaborative Co-manipulation, Humans Have a Motor Behaviour Similar to a Leader

Waldez Gomes, Pauline Maurice,
Jan Babič, Jean-Baptiste Mouret, Serena Ivaldi

Abstract

When two people physically interact to manipulate an object, they synchronize their actions to achieve a common goal. They can agree on a leader and a follower strategy, and cooperate, or combine their efforts without any fixed role agreement, in a collaboration. Previous studies found that interacting partners perform better than individuals and that they can coordinate their movements without explicit role directives, however, is it more effective to use cooperation, or collaboration? Here, agents engaged in a collaboration, making fewer errors than when roles were fixed in a leader/follower format. Furthermore, high values of muscle co-contraction have been associated to leadership roles in the literature, but surprisingly, we observed that both human agents exhibit high values of co-contraction during collaboration. These results clarify the compromise between individual/mutual physical effort against common task execution accuracy that should be taken into account when designing or analyzing human dyadic interactions.

Humans in a dyadic interaction typically organize their movements around non-random, synchronized patterns in both timing and form [1–3]. Many factors may influence dyadic motor behaviour, such as: sensory cues [4]; roles [5]; or skill level to execute a given activity [6]. When the human dyad is haptically coupled, several studies use a leader/follower dichotomy [7–12] to classify the roles of each agent based on haptic signals such as force or stiffness. However, this premise may limit the understanding of the interaction, as recent studies in neurology and psychology domains have reported that humans may see themselves as a dyadic interaction unit "greater than the sum of its parts" [13, 14].

According to Jarrassé *et al.*, physical interactive tasks between dyads (human or robots) can be classified in three categories [5]: competition, collaboration, and cooperation. During a *competition*, the benefit of an agent is detrimental to the other agent, therefore, they may work against each other if necessary. If prior to the task execution, the agents have been assigned, or agreed upon, different roles (assymmetric responsibilities) to execute the task, then the interactive task is classified as a *cooperation*. In contrast, during a *collaboration*, both agents form a coalition to ac-

complish the task [15]. The activity is "synchronized and coordinated in order to build and maintain a shared conception of a problem" [16]. That is, in a collaboration, the agents may deliberate and negotiate their roles in executing the task for the dyad common good.

Human-human dyads within a leader/follower dichotomy are actually a typical case of assymetric role assignment in which the two cooperate to achieve a common goal [5]. Meanwhile, the follower has a completely compliant behavior that only supports the actions of the leader. Many studies have associated this compliance regarding the other agent with different levels of stiffness for trajectory trackings [11,17–20]. For instance, if an agent has a high arm stiffness, then it is less compliant, and it acts as a leader, and vice-versa. However, to the best of our knowledge, no study has investigated the stiffness levels across leader/follower cooperation and collaboration conditions for the same human dyad. If the collaboration condition is where negotiations occur, can we identify a switching between leader and follower roles by looking at each agent's motor behavior? Or particular levels of stiffness that suggest a collaboration is established by the agents? Moreover, if the dyad organization also strongly affects the task execution, it could also have an effect on the task performance.

Our study's goal is, hereafter, threefold. First, to evaluate if leader-follower cooperation, and collaboration conditions affect the stiffness levels of agents in a human dyad during a shared joint task. Secondly, to evaluate if the trajectory of the object being manipulated by the dyad is also affected. And lastly, if there is in fact a variation in performance with respect to a common goal for both agents in the dyad. For this matter, we have designed an object manipulation experiment that requires precise movements, and where a human-dyad is organized in two different leader-follower conditions, as well as in a collaboration condition.

Results

We designed an object manipulation task where two agents need to precisely extract a pipe from one tube without touching the tube's walls (phase 1, extraction), move it around an obstacle (phase 2, free movement), and finally insert it into another tube (phase 3, insertion), again, without touching the walls (Fig. 1a). In all three phases, the agents hold the pipe at the same time, in different grasping locations. Moreover, we defined a common goal for both agents by informing them to control the pipe in order to avoid contacts between the pipe and the walls during phases 1 and 3. In this experiment, the participants executed the task under 3 conditions: 2 conditions for cooperation, with participants being told to act either as a follower or as a leader, and 1 condition for collaboration with no preassigned roles.

Collaboration leads to muscle co-contraction levels as high as in leaders

We calculated an index of co-contraction (ICC) that directly reflects the arm stiffness modulation [21–23] (please, refer to methods section for more

details). In the dyad experiment, we expected that different role assignments to a human dyad would affect each agent's arm stiffness. Then, we estimated an ICC for each agent as the ICC and the arm stiffness are directly proportional. Friedman tests indicated that the ICC RMS value, icc_{rms}, was significantly different between the groups of leaders, followers, and agents in collaboration, $\chi^2(2) = 24.7$, $p < .001$. However, posterior post-hoc Friedman tests revealed that there was no significant difference between the leader icc_{rms} and the collaboration icc_{rms} ($p = .246$) while both of them were significantly different from the follower icc_{rms} ($p = .005$) (fig. 2b).

Since the median of icc_{rms} is the smallest of the 3 conditions, the inferential statistical analysis suggests that the co-contraction was increased both when the human took the leadership, and when he/she collaborated.

Trajectories tend to be deviated toward the dyad's leader

During the leader/follower cooperation, leaders are expected to try to impose their own intended trajectories to the pipe trajectory. We defined a trajectory deviation angle, α, that quantifies how much an agent deviates the dyad trajectory towards him/herself [1]. An analysis of variance with repeated measures was applied to the deviation angle α for the 3 coordination conditions. There was indeed a significant effect on α, ($F(2,18) = 10.85$, $p = .0008$, $\eta^2 = 0.13$) across the experiment conditions, and, Bonferroni corrected post-hoc t-tests showed a significant difference in α between every condition, from collaboration to agent 1 being the leader ($p = .002$), from collaboration to agent 2 being the leader ($p = .001$), and between both cooperation conditions ($p < .0001$). As expected, the median values for all conditions (fig. 3c) suggests that the trajectory of the object deviated towards the agent who was the preassigned leader of the task (fig. 3a). Furthermore, in the collaboration condition, the median of α was between the medians for the other two conditions.

The main dyad experiment also raised the question of how different would the object's trajectory be if the agents were moving the object on their own, and most importantly if the trajectory would still deviate towards the agent when he/she is the only one doing the task, therefore, no partner bias. To answer these questions, we verified the deviation angle of the trajectories per position of the agent (fig. 7b) during the solo experiment. The statistical analysis ($t(49) = 13.06, p < .001, d = 2.59$) showed that the deviation angle does change per position, and the means of the deviation angle, in the solo experiment, showed a more accentuated deviation towards the solo agent than the deviation angle towards the leader agent in the main dyad experiment. Furthermore, the mean values of α for each condition (Fig. 7b) are even greater than on the main dyad experiment when the leaders were in the same positions. This also reinforces our argument that the leaders had an intended trajectory shaped closer to their bodies.

[1] Refer to methods section for more details

Fewer errors during collaboration than during cooperation conditions

Since the contacts were undesired per task definition, every contact at any of the walls is considered as an error committed by the dyad. The medians for every condition suggested that the dyad comitted less errors during collaboration than in cooperation (Fig. 2a). We verified that the different task conditions had a significant effect on the error count for the dyad ($\chi^2(2; 149) = 13.8$, p = .001). Furthermore, Tukey corrected post-hoc tests revealed a significant difference between the collaboration condition and cooperation conditions (when agent 1 was the leader p = .02; and when agent 2 was the leader p = .002), and without any difference between cooperation conditions (p = .67).

In our setup, the seating positions and the grasping handling positions are not symmetric. Depending on the position, each agent has a different view of Tube 1 or Tube 2. This could introduce a bias for errors in one tube or the other depending on how close the tube is to the leader of the task, in the dyad experiment, or the solo agent, in the solo experiment. First, we analyzed if the distance of any of the tubes to the leader in the dyad experiment would have an influence on the number of errors for each tube, and no significant effect was found , $\chi^2(1, 199) = 2.0322$, $p = 0.154$ (Fig. 5). Second, we analyzed if the distance of any of the tubes to the agent in the solo experiment would have an influence on the number of errors for each tube, and once again, no significant effect was found $\chi^2(1, 199) = 1.409$, $p = .24$ (Fig. 7a). Both results indicate, that the better performance for the collaboration condition on the dyad experiment was not biased by our task setup.

Discussion

Our results in the cooperation condition agree with recent research on human dyadic interaction that suggests that when they are not competing, humans try to convey their intended trajectories for the object by modulating their stiffness in the space [4, 24], while also estimating the partner's goal [25, 26]. However, we did not expect that without preassigning leader/follower roles, in a collaboration, the stiffness levels of both agents would be similar to the leaders' stiffness levels. On one hand the agents could have been increasing their stiffness as a result to perceiving the other agent as a disturbance. On the other hand, this could mean that the agents established a bi-directional communication, eventually co-adapting to a trajectory that blends the intended trajectories of both agents.

Whenever there was a leader, the deviation angle, α, indicated a trajectory closer to the leader as it was expected from the literature on obstacle avoidance for humans acting solo [27]. However, during collaboration, the angles indicated trajectories in-between the leadership trajectories for each agent. This suggests that, in their achieved pipe trajectory, the leaders dominated the outcome trajectory, meanwhile, when in collaboration, there was no clear dominance for neither agent. This lack of dominance

throughout the entire task execution discards the possibility that during collaboration there could have been plasticity between leader/follower roles during the task execution [28].

There are already several indications that for individual motion planning the motion is a result of an underlining optimization process that could take into account several kinds of cost functions, such as speed or physical effort [29–34]. So it is not surprising, that the agents would try to minimize the contacts with the walls, especially given it was one of the task pre-defined objectives. On the other hand, it was surprising that the collaboration outcome significantly decreased the number of contacts in comparison to the cooperation conditions. Additionally, in collaboration, each one of the agents had RMS ICC levels on the same high-level as in the preassigned leader conditions, therefore, the overall arm stiffness and muscle effort were also at a high level. So, why did the agents chose a strategy that spends more energy?

There is evidence that while interacting, humans may use the sensorimotor channel to coordinate joint actions [35] among 2 or more agents [26] even if it means increasing the agents' efforts. Some studies have reported that in a shared object manipulation in a situation analogous to the collaboration defined here, the human dyad develops a shared sense of control (capability of an individual to influence the surrounding environment), in opposition to their own sense of agency [13]. Even more, there is already behavioural and neurological evidence that humans visually perceive dyadic interactions differently, and more so, that interacting individuals are seen as a dyad interaction unit rather than separate individuals [14, 36–38]. Hence, it is possible that during collaboration, the agents shifted into a "we-mode" [13] , where they self-coordinated towards a collective target [26], and evaluated the dyad's performance over achieving their own desired trajectories.

Alternatively, Jagau and van Veelen [39] used game theory to model the behaviour of cooperating agents showing that there is a variety of possible strategies that can emerge as a consequence of different combinations of intuition and deliberation, which in the literature are considered as the main drives to explain cooperation. Intuition is the automatic, fast, effortless and often emotional process; deliberation is the rational, controlled, slow and effortful process. Rand [40] explains that "decisions made under time pressure are more heavily influenced by intuition, whereas decisions made under time delay are more heavily influenced by deliberation". In time-constraint studies, where subjects are required to make their decisions quickly before a given amount of time elapses (which is the case of our study), intuitive behaviour is preponderant. This suggests that the increase of co-contraction in the two agents of the dyad could be an intuitive behavioural response influenced by our explicit instructions telling subjects not to make errors and to be fast. Considering that the human motor control literature shows that humans co-contract the arms when moving under physical perturbations [23] it is possible that in the collaboration condition of our experiment the partners were co-contracting because they were considering the other partner as a disturbance rather than an agent whose behaviour is predictable or could be predicted, which is the case of the cooperation condition where the agent knew about the

role of the other partner and therefore could have a prediction of his/her behaviour.

It is reasonable to argue that when in collaboration, both partners seemed to be actively trying to correct each other through its stiffness levels and intended trajectory. Collaboration in a shared haptic task may indeed naturally develop into a role beyond the usual leader/follower dichotomy for dyadic interactions [28, 41]: A collaborator role. This collaborator role would take into account individual environment information, requirements, and expertise from both agents encoded by their intended trajectories to form a more efficient trajectory according to a given *common criteria*, in here, the indication to not touch the tubes' walls. This role may even be the reason why several other studies have reported improvements when executing tasks as a human dyad against executing them alone [6, 42, 43].

Methods

Participants

Two experiments were designed with the same task and setup, but with different configurations regarding the human agents: the main experiment requires a human dyad (Fig. 1a), and a complementary control experiment requires a solo subject (Fig. 6). The dyad experiment was executed by 10 human dyads, therefore 20 participants, of which 15 were male, and 5 were female. Their age ranged from 22 to 38 years old (M = 26.6 years, SD = 3.61 years). 17 participants were right-handed, and 3 were left-handed even though all manipulations were performed with the right hand.

The solo experiment was executed by 10 solo participants, of which 9 were male, and 1 was female. Their age ranged from 22 to 32 years old (M = 25.7 years, SD = 2.16 years). 2 subjects were left-handed. Participants from the dyad experiment did not participate on the solo experiment and vice-versa.

Every participant provided written informed consent for their participation in the experiment. No participant claimed any chronic motor disease or health condition that could influence in the experiment's results. The experiments were approved by INRIA's ethical committee (COERLE).

Task Description

The task consists in manipulating an object (pipe) to bring it from a start to an end point (Fig. 1a). The participants are instructed to avoid moving their back during the task execution (they are not strapped). They hold the pipe with their right hand with a power grasp, placing their hand on one of the designated handles. In the start (Phase 1), the pipe is within Tube 1 (the one closest to Agent 1), then the pipe has to be taken out of Tube 1 while avoiding contact with Tube 1's front wall. After extracting the pipe from the tube (Phase 2, free movement), the pipe has to be moved around a cylindrical obstacle towards Tube 2 (the one closest to Agent 2).

Then, the pipe has to be inserted into Tube 2 (Phase 3) [2], while avoiding contact with the front wall. By design, the task is always recorded and evaluated from Tube 1 to Tube 2, and the return motion is ignored.

Even though there is no physical restriction on the pipe's motion after exiting Tube 1 and before entering Tube 2, the agent(s) are told not to move the pipe over the cylindrical obstacle. Effectively, this enforces a planar movement of the pipe.

If two human agents execute the experiment, then a black curtain is placed between the participants to prevent visual contact between their faces during the task execution. In addition, they are instructed not to talk during the task execution. These measures restrict the dyad communication almost exclusively to the haptic channel provided by the physical interaction.

Duration

During the task execution, none of the agents saw a timer, but they were told that the whole manipulation (from Start to End) should not last longer than 15 s. If participants took significantly longer than 15 s then they were told so and the trial was canceled.

Apparatus

The manipulated object is a 218 g pipe of diameter 3 cm and length 50 cm, with 10 cm wide handling areas for both agents. One end of the pipe is covered with 8 cm long of aluminum foil, which makes it possible to detect whenever the pipe touches any of the tube walls. On the other hand, since the tubes are 10 cm long, it is impossible to detect a contact between the front and back walls of a tube at the same time.

Experiment Description

Dyad experiment

In the *dyad* experiment, two agents shared the pipe manipulation. Each agent sat on one side of the table (Agent 1 and Agent 2 in Fig. 1a). Two handles were drawn on the pipe: Agent 1 held the pipe on Handle 1 (blue in Fig. 1a), while Agent 2 held the pipe on Handle 2 (green in Fig. 1a). The Agents did not switch seat position, *i.e.* one Agent was always Agent 1, and the other always Agent 2. Participants performed the task in 3 different conditions:

- *No specified roles:* Agents were only instructed to manipulate the pipe;
- *Agent 1 Leader and Agent 2 Follower:* Participants were instructed that Agent 1 must lead the movement, while Agent 2 was only there to support and follow Agent 1;

[2] For the calculations of the instant between transitions, refer to the supplementary material

- *Agent 1 Follower and Agent 2 Leader:* Participants were instructed that Agent 2 must lead the movement, while Agent 1 is only there to support and follow Agent 2.

The order of the 3 conditions was randomized across dyads to counter-balance possible biases.

Before starting the recording for each condition the participants could practice for 2 trials. For each condition, 5 trials were recorded, resulting in a total of 15 trials. Since there were 10 recorded dyads, a total of 150 trials were recorded among all dyads.

There was an approximate 45 s break between each trial, but the exact duration of the break was not imposed (participants decided when they wanted to start the next trial).

Solo experiment

In the *solo* experiment, there was only 1 agent (Fig. 6). The Agent held the pipe between Handle 1 and Handle 2. There were 2 conditions in the *single* experiment:

- *Position 1:* The participant sat in Agent 1's position;
- *Position 2:* The participant sat in Agent 2's position.

The order of the 2 conditions was randomized across participants to counter-balance biases.

Agents performed 5 trials for each condition, and 10 trials in total. Similarly to the *dyad* experiment, the trials were separated by an approximate 45 s break, and 2 practice trials were allowed at the beginning of each condition.

Data Collection

During both experiments, we gathered data on each agent's arm, motion and muscle activity. And to assess how accurate the agent (or the dyad) was in executing the task, we also measured how many times the pipes would touch the tube walls.

Motion capture

The motion of the participants' right arm was recorded with a Qualisys optical motion capture system (at rate of 150 Hz). Four reflective markers were placed on the participant's hand to track their 3D Cartesian positions:

- 1 marker on the Ulnar-Styloid Process
- 1 marker on the Head of the 5th Metacarpal
- 1 marker on the Head of the 2nd Metacarpal
- 1 marker on the Radial-Styloid Process

In addition, 5 markers were placed on the pipe, tubes and obstacle:

- 1 at the tip of the pipe which does not go inside the tubes (opposite to where the aluminum foil is). Agents were told to hold the pipe so that this marker was facing up (referred to as *pipe*);
- 1 at the top of the front wall of each tube (referred to as *tube1* and *tube2*);
- 1 at the top of the obstacle wall, farthest away from both tubes (referred to as *obsTop*);
- 1 at the bottom of the obstacle wall, farthest away from both tubes (referred to as *obsBot*);

Electromyography

In the *dyad* experiment, 6 wireless Delsys Trigno EMG sensors were placed on the participant's right arm, on the following muscles:

- Flexor Carpi Ulnaris;
- Extensor Carpi Ulnaris;
- Biceps Brachii;
- Triceps (lateral head);
- Deltoid, Anterior;
- Deltoid, Posterior.

The EMG sensors are placed on the subject following guidance rules from the European project SENIAM [44], as well as location cues from Perroto, 2011 [45]. After we have located a muscle, the subject is asked to contract it to confirm the location of the "muscle belly", that is then marked with a pen. For each muscle, an EMG sensor is assigned, and annotated in our EMG acquisition software.

Before placing a sensor on a muscle location, the area surrounding the pen mark is prepared accordingly. The subject's skin is cleaned with alcohol until it acquires red tones, which indicates good skin impedance. After the alcohol dryes out, the EMG sensor is placed on the skin at the muscle fibers direction with the help of a double-sided sticker provided by the sensor manufacturer.

Prior to the task execution, each agent is asked to perform maximum voluntary contractions (MVC) during isometric exercises for each selected muscle [44] for 3 s. The exercise is performed 3 times, with a 1 minute interval between them to decrease fatigue biases. After the 3 trials, the maximum EMG signal is then stored and used for posterior post-processing of the EMG signals during the task execution.

Contacts

The designed task requires the solo agent, or human dyad, to avoid contact between the pipe and the tube walls. We then use contact sensors to detect those contacts, and posteriorly use this information as a performance measure.

To detect the contacts between the pipe and the tubes, we wrapped the end of the pipe with aluminum foil, and metallic rings were placed inside

the walls of both tubes. Those contact sensors are essentially mechanical switches which are known for their bouncy signals, so to circumvent this issue we debounce the input through our software. After we detect a signal onset (a contact) no other onset is stored as a contact for the next 100 ms window (roughly half of the average human simple reaction time [46]).

Data Processing and Analysis

EMG Processing

Surface EMG signals are easy to capture, but require careful pre-processing before analysis [47]. Here, the EMG signal for the i-th muscle, u_i, was passed through a 100 ms RMS window, and filtered by a low-pass third order Butterworth filter with a 10 Hz cutoff frequency to generate a filtered signal u_i^{fil}. However, the filtered signal alone is only proportional to its respective muscle activation, or contraction.

To obtain an index of the muscle activation, between 0 and 1, we needed to normalize the signal with respect to its stored MVC value:

$$u_i^{norm} = \frac{u_i^{fil}}{u_i^{MVC}} \tag{1}$$

, where u_i^{norm} can finally be used to provide information on the arm stiffness modulation.

Index of Co-Contraction

Instead of generating movement at a given joint, equivalent contraction from antagonist muscles tend to increase joint stiffness. Given the activation levels from two antagonist muscles, i, j, we can calculate an index of Co-Contraction for their respective k joint [21–23]:

$$icc_k(t) = min(u_{norm}^i(t), u_{norm}^j(t)) \tag{2}$$

, where $icc_k(t) \in [0, 1]$.

In both experiments, we processed the EMG signals from only two antagonist muscles with respect to the wrist joint movement (Flexor Carpi Ulnaris and Extensor Carpi Ulnaris). Due to muscle synergy [48], the *icc* for both muscles should reflect the arm stiffness modulation for the entire arm. To simplify the notation, we refer to the *icc* corresponding to both of those muscles as ICC.

Deviation Angle α

From obstacle avoidance motor planning, we expected humans to plan their arm trajectories while taking into account inertial and kinematic properties of their arms, likely favoring motion plans with their hands closer to their bodies [27]. During a leader/follower cooperation, leaders were expected to try to impose their own intended trajectories to the pipe trajectory. Therefore, since in our case the agents were seated facing each other (Fig. 1a), we expected the intended leader trajectories to be different from the follower trajectories. In the cooperation scenario, the

resulting pipe trajectory should have roughly translated to the intended leader trajectory [3], however, there was no clear expectation for what could have happened in the collaboration scenario.

To quantify how the pipe trajectories favor one agent or another, we defined a trajectory deviation angle α. Positive values of α mean that the trajectory deviates towards agent 1, and negative values mean deviation towards agent 2 (fig. 3b). Specifically, α quantifies the skewness of the pipe trajectory with respect to the Y-axis that divides the experimental setup symmetrically. Given a dyad or agent's hand markers centroid trajectory, $\vec{r}(t)$, we calculated the point in which the position is maximum in the Y-axis

$$t_{max} = \arg\max(r_y) \tag{3}$$

$$\vec{r}_{max} = \vec{r}(t_{max}) \tag{4}$$

and the position of the marker in front of the obstacle $\vec{r}_{obs}$ to be able to calculate a vector that indicates the direction of the skew.

$$\vec{r}_{dir} = \vec{r}_{max} - \vec{r}_{obs} \tag{5}$$

Then, α is the smallest angle between the Y-Axis vector and $\vec{r}_{dir}$.

Statistical Analysis

Index of Co-Contraction

Each agent's ICC is in fact a time series, however, for the purpose of this study, we decided to obtain a representative value of the ICC for every task execution calculating an RMS value. In addition, during phases 1 and 3 of the task, while the pipe is within any of the tubes, the agents have to act more precisely to avoid contacting the tube walls, so it is likely that there will ne more co-contraction than is phase 2. Therefore, we decided to calculate the RMS value, icc_{rms}, only for the phases 1 and 3 of every task execution.

In the dyad experiment, there is 1 source of icc_{rms} data from each agent. To evaluate the effect of the roles on the RMS values, we re-grouped them into 3 new conditions: icc_{rms} of a leader, icc_{rms} of a follower, and icc_{rms} during collaboration without pre-assigned leadership. Since there were 5 trials per dyad and 2 agents per dyad, each role condition included 10 ICC measurements, therefore, 30 measurements per dyad, and 300 in total. Finally, for the statistical analysis in the *dyad* experiment, since the ICC data was not Gaussian (Shapiro tests with $p < 0.001$), the median for each new condition was calculated in order to enable the usage of Friedman tests.

Deviation Angle Data

The deviation angle in both experiments had a normal distribution (Shapiro-Wilk normality test (Dyad manipulation: p = .39; Solo Manipu-

[3] Refer to supplementary material for all resulting trajectories

lation: p = .05)), therefore, a regular analysis of variance with repeated measures (or a paired t-test for the solo experiment) was done to verify the effect of the conditions on the deviation angle.

Contact Sensor Data

The data from the contact sensors is made of natural numbers, therefore, the sample measures are in fact classified as *count data*. After verifying that the count data was overdispersed (variances larger than means) in both experiments, we used a general linear mixed model with negative binomial distributions [49], with random effects to account for the repetitions in the same condition. Since there are 3 conditions, post-hoc tests with Tukey correction were used to evaluate if the different conditions affected the number of contacts.

Data Availability

The raw data for EMG signal, motion measurements, and number of wall touches is freely available in Zenodo at the DOI: 10.5281/zenodo.3989616 [50].

Code Availability

The custom code used to obtain the MVC values for the EMG signals can be found on `http://github.com/inria-larsen/emg-processing`.

References

[1] Frank J. Bernieri and Robert Rosenthal. Interpersonal coordination: Behavior matching and interactional synchrony. 1991.

[2] David P. Black, Michael A. Riley, and Christopher K. McCord. Synergies in intra- and interpersonal interlimb rhythmic coordination. *Motor Control*, 11(4):348 – 373, 2007.

[3] R.C. Schmidt, Paula Fitzpatrick, Robert Caron, and Joanna Mergeche. Understanding social motor coordination. *Human Movement Science*, 30(5):834 – 845, 2011.

[4] Keivan Mojtahedi, Bryan Whitsell, Panagiotis Artemiadis, and Marco Santello. Communication and inference of intended movement direction during human–human physical interaction. *Frontiers in Neurorobotics*, 11:21, 2017.

[5] Nathanaël Jarrasse, Themistoklis Charalambous, and Etienne Burdet. A framework to describe, analyze and generate interactive motor behaviors. *PLOS ONE*, 7(11):1–13, 11 2012.

[6] S. Kager, A. Hussain, A. Cherpin, A. Melendez-Calderon, A. Takagi, S. Endo, E. Burdet, S. Hirche, M. H. Ang, and D. Campolo. The effect of skill level matching in dyadic interaction on learning of a tracing task. In *2019 IEEE 16th International Conference on Rehabilitation Robotics (ICORR)*, pages 824–829, 2019.

[7] A. Melendez-Calderon, V. Komisar, G. Ganesh, and E. Burdet. Classification of strategies for disturbance attenuation in human-human collaborative tasks. In *2011 Annual International Conference of the IEEE Engineering in Medicine and Biology Society*, pages 2364–2367, Aug 2011.

[8] Lucia Maria Sacheli, Emmanuele Tidoni, Enea Francesco Pavone, Salvatore Maria Aglioti, and Matteo Candidi. Kinematics fingerprints of leader and follower role-taking during cooperative joint actions. *Experimental Brain Research*, 226(4):473–486, May 2013.

[9] R. Groten, D. Feth, R. L. Klatzky, and A. Peer. The role of haptic feedback for the integration of intentions in shared task execution. *IEEE Transactions on Haptics*, 6(1):94–105, First 2013.

[10] N. Stefanov, A. Peer, and M. Buss. Role determination in human-human interaction. In *World Haptics 2009 - Third Joint EuroHaptics conference and Symposium on Haptic Interfaces for Virtual Environment and Teleoperator Systems*, pages 51–56, March 2009.

[11] C. E. Madan, A. Kucukyilmaz, T. M. Sezgin, and C. Basdogan. Recognition of haptic interaction patterns in dyadic joint object manipulation. *IEEE Transactions on Haptics*, 8(1):54–66, Jan 2015.

[12] A. Melendez-Calderon, V. Komisar, and E. Burdet. Interpersonal strategies for disturbance attenuation during a rhythmic joint motor action. 147:348–358, 2015. Exported from https://app.dimensions.ai on 2019/01/26.

[13] John A. Dewey, Elisabeth Pacherie, and Guenther Knoblich. The phenomenology of controlling a moving object with another person. *Cognition*, 132(3):383 – 397, 2014.

[14] Jon Walbrin and Kami Koldewyn. Dyadic interaction processing in the posterior temporal cortex. *NeuroImage*, 198:296 – 302, 2019.

[15] Pierre Dillenbourg, Sanna Järvelä, and Frank Fischer. The evolution of research on computer-supported collaborative learning. In *Technology-enhanced learning*, pages 3–19. Springer, 2009.

[16] Jeremy Roschelle and Stephanie D Teasley. The construction of shared knowledge in collaborative problem solving. In *Computer supported collaborative learning*, pages 69–97. Springer, 1995.

[17] Alexander Mörtl, Martin Lawitzky, Ayse Kucukyilmaz, Metin Sezgin, Cagatay Basdogan, and Sandra Hirche. The role of roles: Physical cooperation between humans and robots. *The International Journal of Robotics Research*, 31(13):1656–1674, 2012.

[18] Antoine Bussy, Abderrahmane Kheddar, André Crosnier, and François Keith. Human-humanoid haptic joint object transportation case study. In *2012 IEEE/RSJ International Conference on Intelligent Robots and Systems*, pages 3633–3638. IEEE, 2012.

[19] Don Joven Agravante, Andrea Cherubini, Alexander Sherikov, Pierre-Brice Wieber, and Abderrahmane Kheddar. Human-humanoid collaborative carrying. *IEEE Transactions on Robotics*, 35(4):833–846, 2019.

[20] Y. Li, K. P. Tee, R. Yan, W. L. Chan, and Y. Wu. A framework of human–robot coordination based on game theory and policy iteration. *IEEE Transactions on Robotics*, 32(6):1408–1418, 2016.

[21] Kurt A. Thoroughman and Reza Shadmehr. Electromyographic correlates of learning an internal model of reaching movements. *Journal of Neuroscience*, 19(19):8573–8588, 1999.

[22] Paul L. Gribble, Lucy I. Mullin, Nicholas Cothros, and Andrew Mattar. Role of cocontraction in arm movement accuracy. *Journal of Neurophysiology*, 89(5):2396–2405, 2003.

[23] E Burdet, R Osu, DW Franklin, TE Milner, and M Kawato. The central nervous system stabilizes unstable dynamics by learning optimal impedance. *NATURE*, 414:446–449, 2001.

[24] Atsushi Takagi, Francesco Usai, Gowrishankar Ganesh, Vittorio Sanguineti, and Etienne Burdet. Haptic communication between humans is tuned by the hard or soft mechanics of interaction. *PLOS Computational Biology*, 14(3):1–17, 03 2018.

[25] Atsushi Takagi, Gowrishankar Ganesh, Toshinori Yoshioka, Mitsuo Kawato, and Etienne Burdet. Physically interacting individuals estimate the partner's goal to enhance their movements. *Nature Human Behaviour*, 1:0054 EP –, Mar 2017. Letter.

[26] Atsushi Takagi, Masaya Hirashima, Daichi Nozaki, and Etienne Burdet. Individuals physically interacting in a group rapidly coordinate their movement by estimating the collective goal. *Elife*, 8:e41328, 2019.

[27] Philip N. Sabes and Michael I. Jordan. Obstacle avoidance and a perturbation sensitivity model for motor planning. *Journal of Neuroscience*, 17(18):7119–7128, 1997.

[28] Shinnosuke Nakayama, Manuel Ruiz Marín, Maximo Camacho, and Maurizio Porfiri. Plasticity in leader–follower roles in human teams. *Scientific Reports*, 7(1):14562, 2017.

[29] T Flash and N Hogan. The coordination of arm movements: an experimentally confirmed mathematical model. *Journal of Neuroscience*, 5(7):1688–1703, 1985.

[30] Serena Ivaldi, Olivier Sigaud, Bastien Berret, and Francesco Nori. From humans to humanoids: The optimal control framework. *Paladyn*, 3(2):75–91, Jun 2012.

[31] Yasuhiro Wada, Yuichi Kaneko, Eri Nakano, Rieko Osu, and Mitsuo Kawato. Quantitative examinations for multi joint arm trajectory planning—using a robust calculation algorithm of the minimum commanded torque change trajectory. *Neural Networks*, 14(4):381 – 393, 2001.

[32] Y. Uno, M. Kawato, and R. Suzuki. Formation and control of optimal trajectory in human multijoint arm movement. *Biological Cybernetics*, 61(2):89–101, Jun 1989.

[33] Christopher M. Harris and Daniel M. Wolpert. Signal-dependent noise determines motor planning. *Nature*, 394:780 EP –, Aug 1998.

[34] Luka Peternel, Olivier Sigaud, and Jan Babič. Unifying speed-accuracy trade-off and cost-benefit trade-off in human reaching movements. *Frontiers in Human Neuroscience*, 11:615, 2017.

[35] Cordula Vesper, Laura Schmitz, Lou Safra, Natalie Sebanz, and Günther Knoblich. The role of shared visual information for joint action coordination. *Cognition*, 153:118–123, 2016.

[36] Jon Walbrin, Paul Downing, and Kami Koldewyn. Neural responses to visually observed social interactions. *Neuropsychologia*, 112:31 – 39, 2018.

[37] Liuba Papeo, Timo Stein, and Salvador Soto-Faraco. The two-body inversion effect. *Psychological Science*, 28(3):369–379, 2017.

[38] Susanne Quadflieg and Kami Koldewyn. The neuroscience of people watching: how the human brain makes sense of other people's encounters. *Annals of the New York Academy of Sciences*, 1396(1):166–182, 2017.

[39] Stephan Jagau and Matthijs van Veelen. A general evolutionary framework for the role of intuition and deliberation in cooperation. *Nature Human Behaviour*, 1(8):1–6, 2017.

[40] David G Rand. Cooperation, fast and slow: Meta-analytic evidence for a theory of social heuristics and self-interested deliberation. *Psychological science*, 27(9):1192–1206, 2016.

[41] C. Messeri, A. M. Zanchettin, P. Rocco, E. Gianotti, A. Chirico, S. Magoni, and A. Gaggioli. On the effects of leader-follower roles in dyadic human-robot synchronisation. *IEEE Transactions on Cognitive and Developmental Systems*, pages 1–1, 2020.

[42] G. Ganesh, A. Takagi, R. Osu, T. Yoshioka, M. Kawato, and E. Burdet. Two is better than one: Physical interactions improve motor performance in humans. *Scientific Reports*, 4(1):3824, Jan 2014.

[43] K. B. Reed, M. Peshkin, and M. J. Hartmann. Haptic cooperation between people, and between people and machines, 2006.

[44] D Stegeman and H Hermens. Standards for surface electromyography: The european project surface emg for non-invasive assessment of muscles (seniam). 2007.

[45] Aldo O Perotto. *Anatomical guide for the electromyographer: the limbs and trunk*. Charles C Thomas Publisher, 2011.

[46] D. Woods, John M. Wyma, E. Yund, T. Herron, and B. Reed. Factors influencing the latency of simple reaction time. *Frontiers in Human Neuroscience*, 9, 2015.

[47] Carlo J. De Luca. The use of surface electromyography in biomechanics. *Journal of Applied Biomechanics*, 13(2):135–163, 1997.

[48] Mark Ison and Panagiotis Artemiadis. The role of muscle synergies in myoelectric control: trends and challenges for simultaneous multifunction control. *Journal of Neural Engineering*, 11(5):051001, 2014.

[49] A. Colin Cameron and Pravin K. Trivedi. *Regression Analysis of Count Data*. Econometric Society Monographs. Cambridge University Press, 2 edition, 2013.

[50] Waldez Gomes, Pauline Maurice, and Serena Ivaldi. Andy data - human human object co-manipulation, August 2020. Dataset available at https://doi.org/10.5281/zenodo.3989616.

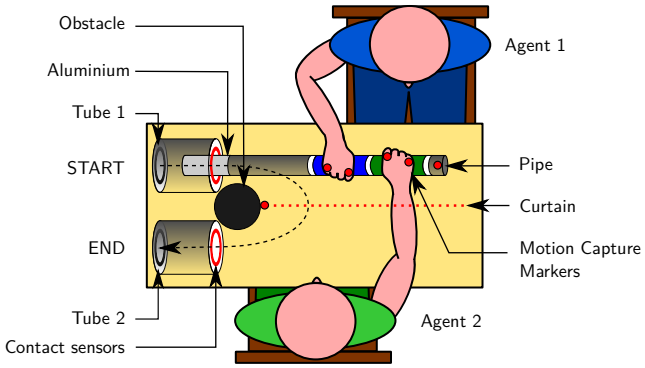

(a)

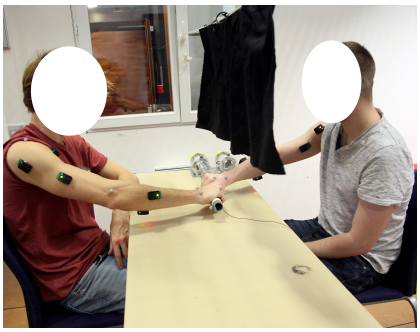

(b)

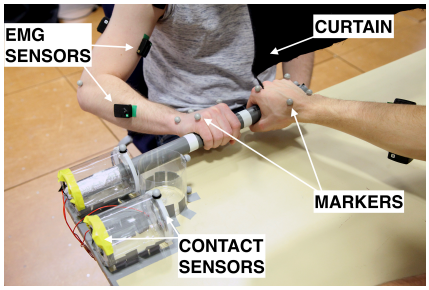

(c)

Figure 1: Experimental Setup. a) **Object co-manipulation by human dyad**: Top-down view of the experiment set-up. The black dashed line approximates the pipe trajectory. The red circles are metal rings attached to the walls of the tubes in order to detect contact with the aluminium that is wrapped around the end of the pipe. The red dashed line represents a curtain placed between both agents to prevent visual communication. b) **Experimental scenario:** Two interacting agents performing the co-manipulation task. A black curtain blocks visual communication between agents. c) **Sensors:** surface EMG sensors placed on the agents' arms, motion tracking markers (on the agents' arms, the pipe, the obstacle, the targets) and contact sensors inside the tubes.

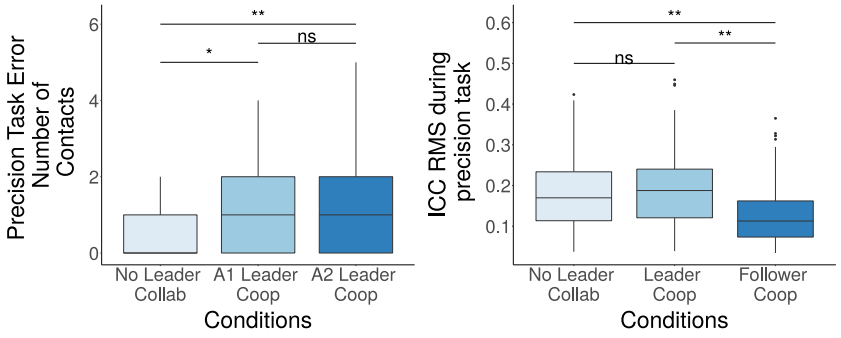

(a) (b)

Figure 2: Both agents increase their muscle co-contraction in the collaboration condition when the trajectory execution is more precise which is when the pipe is within any of the tubes. a) Number of contact errors in the tube walls per condition: No significant difference in the number of contact errors is found between the cooperation conditions, but there is a significant difference in the number of contact errors for both of them and the collaboration condition; b) Root Mean Square index of co-contraction removing and inserting the pipe inside the tube for every condition: Collaboration condition (no leader) is not significantly different from the leader condition, however, both of them are different from the follower condition

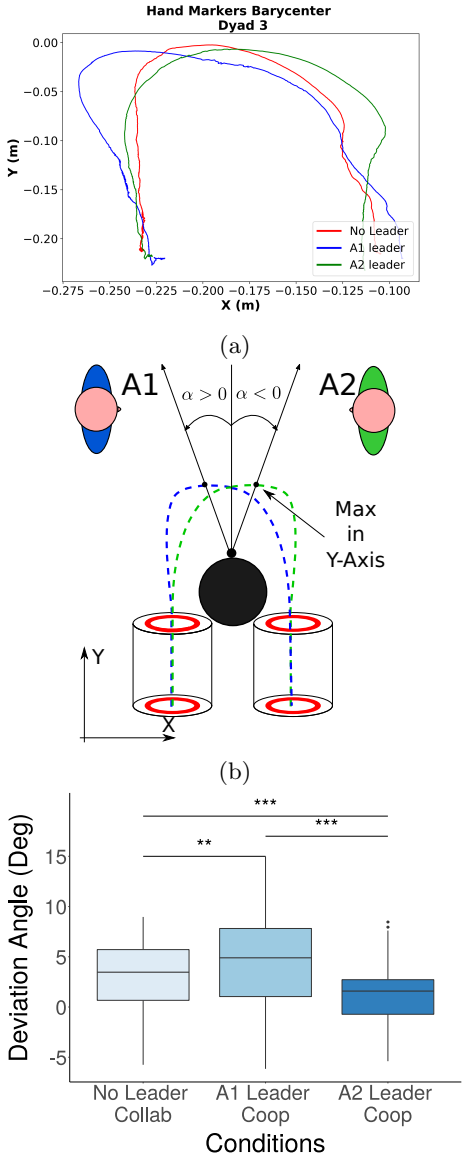

Figure 3: a) Typical trajectories for the different conditions executed by one of the dyads in the experiment (dyad 3); b) Angle of trajectory deviation, α: it is the angle between the vertical line that divides the setup symmetrically, and the line from the obstacle marker to the point of the trajectory with maximum value in the Y-Axis; c) Deviation angle per condition: as can be seen by the median values, during cooperation, the deviation angle α exhibited extreme values towards the leader of the task, and in collaboration, α had values in the middle of those extremes

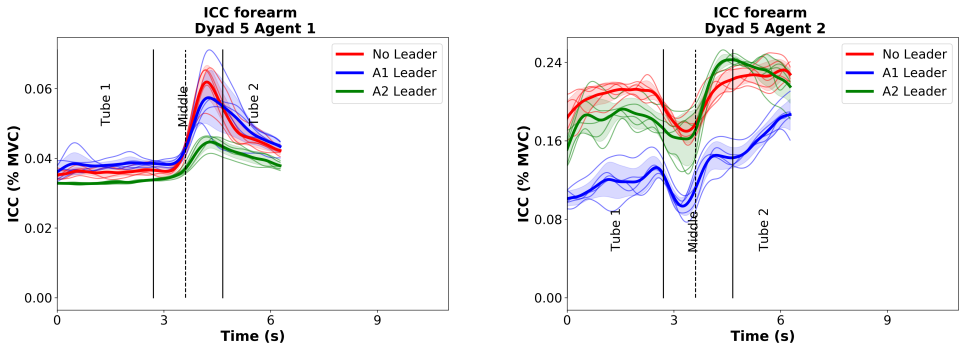

(a) (b)

Figure 4: Index of Co-Contraction (ICC) for the muscle pair Extensor/Flexor Carpi Ulnaris at the subject's forearms, for both agents in dyad 5 of the main dyad experiment.

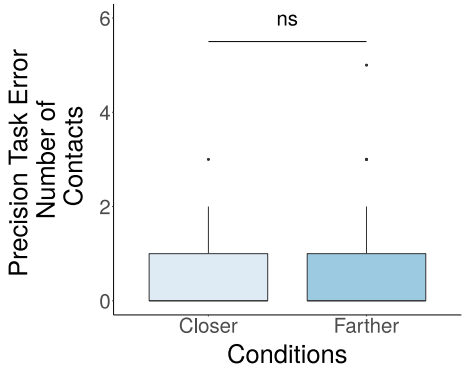

Figure 5: Dyad Manipulation Experiment: Number of touches in the wall, i.e. errors, per tube position w.r.t. the agent. If the agent is on Position 1, Tube 2 is the closer tube, and vice-versa. No significant difference is found between conditions ($p = 0.154$)

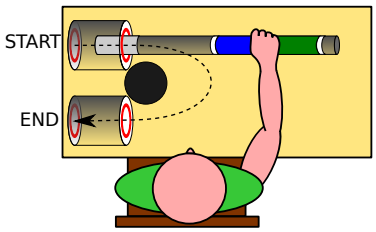

Figure 6: Top down view of the experimental set-up for the Solo Experiment. The human changes position between conditions.

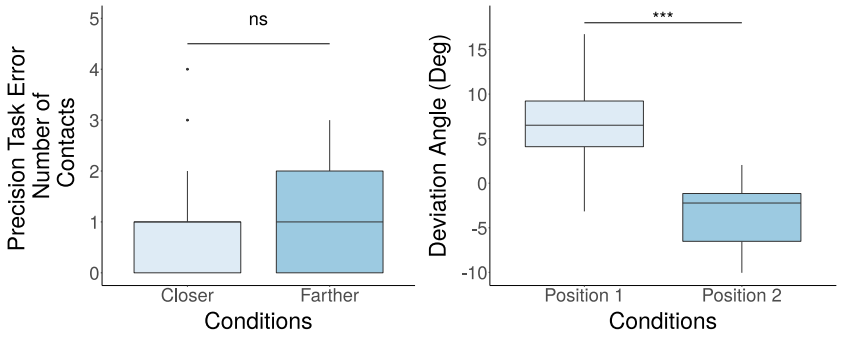

(a) (b)

Figure 7: **Solo Manipulation Experiment**: a) Number of touches in the wall, i.e. errors, per tube position w.r.t. the agent. If the agent is on Position 1, Tube 2 is the closer tube, and vice-versa. No significant difference is found between conditions ($p = .24$) which suggests that number of errors in each tube was not biased w.r.t. agent's position. b) Solo Manipulation Experiment: Deviation angle α per agent position. The agent in position 1 deviates the object trajectory position 1 ($\bar{\alpha} > 0$), and agent 2 deviates its trajectory towards position 2 ($\bar{\alpha} < 0$)

Supplementary Material to "In a Collaborative Co-manipulation, Humans Have a Motor Behaviour Similar to a Leader"

Waldez Gomes, Pauline Maurice,
Jan Babič, Jean-Baptiste Mouret, Serena Ivaldi

Contents

1 Task description

The experiment consists in manipulating an object (pipe) to bring it from a start to an end point (Fig. 1). The experiment starts with the pipe within a tube (Tube 1). First the pipe is taken out of Tube 1, and contact with the wall of the tube should be avoided. Then, the pipe is moved around an obstacle to the entrance of a second tube (Tube 2). Finally, the pipe is inserted inside Tube 2, and contact with the wall of Tube 2 should be avoided.The motion is always performed from Tube 1 to Tube 2. The return motion is not recorded nor evaluated.

While in free space (after exiting Tube 1 and before entering Tube 2), there is no physical restriction on the tube motion. However agents are told to move the obstacle around, and not above.

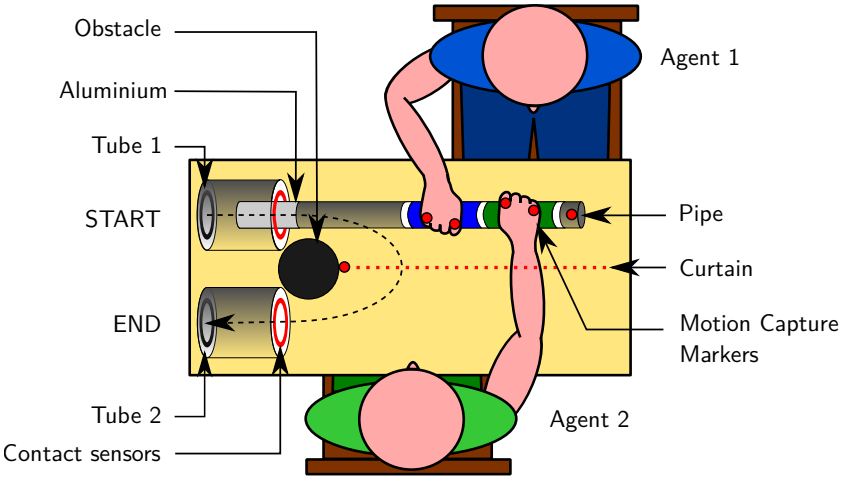

(a)

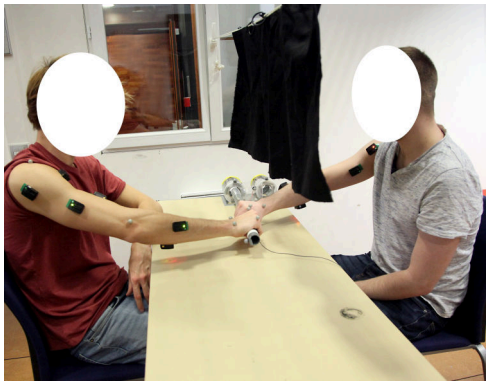

(b)

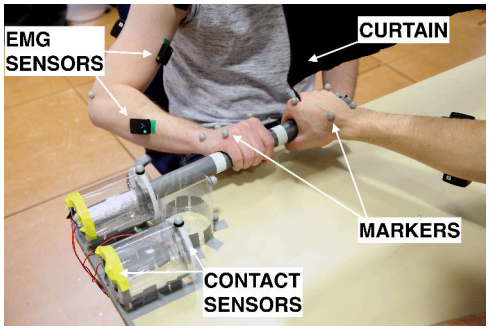

(c)

Figure 1: Experimental Setup. a) **Object co-manipulation by human dyad**: Top-down view of the experiment set-up. The black dashed line approximates the pipe trajectory. The red circles are metal rings attached to the walls of the tubes in order to detect contact with the aluminium that is wrapped around the end of the pipe. The red dashed line represents a curtain placed between both agents to prevent visual communication. b) **Experimental scenario:** Two interacting agents performing the co-manipulation task. A black curtain blocks visual communication between agents. c) **Sensors:** surface EMG sensors placed on the agents' arms, motion tracking markers (on the agents' arms, the pipe, the obstacle, the targets) and contact sensors inside the tubes.

1.1 Duration

The task starts with a contact on the back wall of Tube 1 and ends with a contact on the back wall of Tube 2 (back walls are the farthest walls from participants). These initial contacts are used to indicate the start and end of the manipulation. Participants do not see any timer during the experiment, but they are told that the whole manipulation (from Start to End) should not last longer than 15 s. If participants take significantly longer, they are told so and the trial is canceled (In all trials the mean duration was 8.68 s, with a standard deviation of 3.04 s).

1.2 Object

The object that is manipulated is a pipe of diameter 3 cm and length 50 cm (Fig. 2). Each handle is 10 cm wide. The part covered with aluminum foil is 8 cm long, so that it is impossible to detect a contact with the front and back walls of a tube at the same time. The pipe weighs 218 g

Each tube is 10 cm long, with a diameter of 8 cm. The diameter of the holes in the front and back walls of each tube is 4.5 cm. The obstacle is a vertical transparent cylinder of diameter 8 cm. Both tubes are set 13 cm apart (distance between the centers of the tubes).

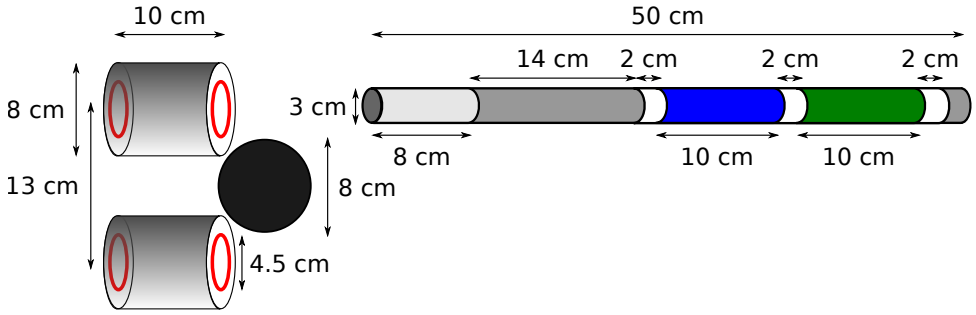

Figure 2: Dimensions of the pipe and tubes.

1.3 Instructions to the Participants

Each participant is seated on a chair, with one chair on each side of the table. Before the experiment, participants can adjust the chair position to find a comfortable position. Participants are instructed to avoid moving their back during the task execution (they are not strapped). They hold the pipe with their right hand with a power grasp, placing their hand on one of the designated handles.

A curtain is placed between both agents to prevent visual contact during the task execution. Participants are instructed not to talk during the task execution, and not to talk about the experiment between trials.

2 Experimental design

In this study, two experiments were designed with the same setup: the first is the dyad experiment where a human dyad manipulates the object; The second is the solo experiment executed by one human participant. The latter was designed to verify if there was any bias on the dyad experiment regarding the position of the human agents.

2.1 Dyad experiment

In the *dyad* experiment, two agents manipulate the pipe together. Each agent seats on one side of the table (Agent 1 and Agent 2 in Fig. 1). Two handles are drawn on the pipe: Agent 1 holds the pipe on Handle 1 (blue in Fig. 1), while Agent 2 holds the pipe on Handle 2 (green in Fig. 1). The participants do not switch seat position, *i.e.* one agent is always Agent 1, and the other always Agent 2. Agents perform the task in 3 different conditions:

- *Collaboration (Natural Behaviour):* Participants are instructed to manipulate the pipe as naturally as possible (marked as *Cond_0L* in the data files);
- *Agent 1 Leader and Agent 2 Follower (Constrained Behaviour):* Participants are instructed that Agent 1 must lead the movement, while Agent 2 is only here to support and follow Agent 1 (marked as *Cond_1L* in the data files);
- *Agent 1 Follower and Agent 2 Leader (Constrained Behaviour):* Participants are instructed that Agent 2 must lead the movement, while Agent 1 is only here to support and follow Agent 2 (marked as *Cond_2L* in the data files).

The order of the 3 conditions is randomized across dyads to counter-balance possible biases.

Agents perform 5 trials for each condition, resulting in a total of 15 trials. For each of the 3 conditions, before starting the recording the agents can practice for at least 2 trials. There is an approximate 45 s break between each trial, but the exact duration of the break is not imposed (agents decide when they want to start the next trial).

2.2 Solo experiment

In the *solo* experiment, the solo agent manipulates the pipe alone. The agent holds the pipe on the middle of Handle 1 and Handle 2. There are 2 conditions in the *solo* experiment:

- *Position 1:* The participant seats in Agent 1's position (marked as *Cond_S1* in the data files);
- *Position 2:* The participant seats in Agent 2's position (marked as *Cond_S2* in the data files).

The order of the 2 conditions is randomized across participants to counter-balance possible biases.

Agents perform 5 trials for each condition, for a total of 10 trials. Trials are separated by an approximate 45 s break, and 2 to 3 practice trials are allowed at the beginning of each condition. Note that in the data files, trials are numbered from 1 to 10 (1 to 5 being the first condition and 6 to 10 the second condition).

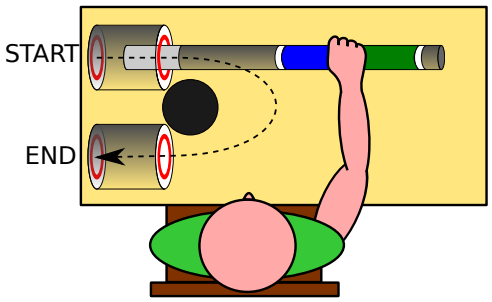

Figure 3: Top down view of the experimental set-up for the Solo Experiment. The human change position between conditions.

3 Measurements

Figure 4 summarizes the equipments used to acquire data for this experiment. The windows laptop synchronizes the data acquisition from Qualysis and Delsys through their proprietary software. The Linux laptop is used to collect data from the contact sensor, and additionally executes a graphical interface for acquisition of EMG maximum voluntary contractions (MVC) [1].

3.1 Motion capture

The motion of the participants' right arm is recorded with a Qualisys optical motion capture system. 4 reflective markers are placed on the participant's hand, and their 3D Cartesian positions are tracked. The position of the 4 markers are (Fig. 5):

- 1 on the Ulnar-Styloid Process (referred to as *Hand1* in the kinematics data files);
- 1 on the Head of the 5th Metacarpal (referred to as *Hand2* in the kinematics data files);
- 1 on the Head of the 2nd Metacarpal (referred to as *Hand3* in the kinematics data files);
- 1 on the Radial-Styloid Process (referred to as *Hand4* in the kinematics data files).

In addition, 5 markers are placed on the pipe, tubes and obstacle (Fig. 5):

- 1 at the tip of the pipe which does not go inside the tubes (opposite to where the aluminum foil is). Agents were told to hold the pipe so that this marker was facing up (referred to as *pipe* in the kinematics data files);

[1] This GUI can be found in: https://github.com/inria-larsen/emg-processing

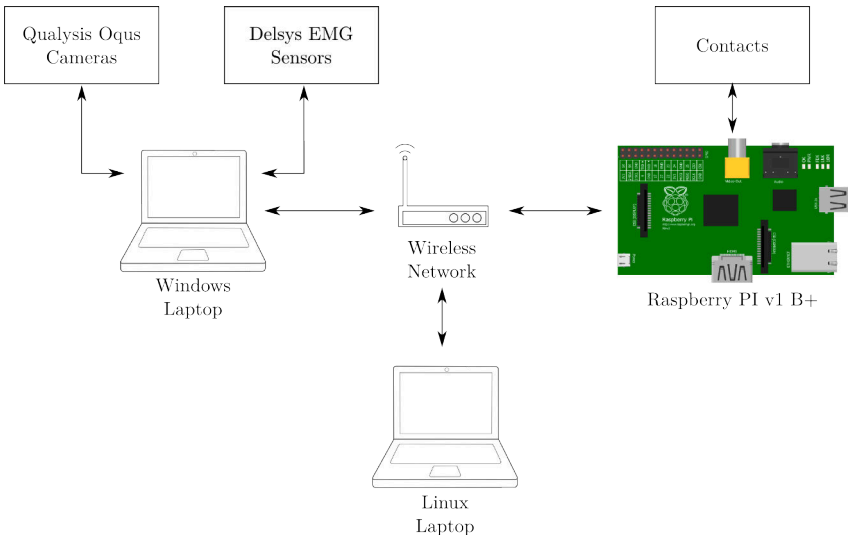

Figure 4: Diagram with the sensors and equipment used for data collection.

- 1 at the top of the front wall of each tube (referred to as *tube1* and *tube2* in the kinematics data files);
- 1 at the top of the obstacle wall, farthest away from both tubes (referred to as *obsTop* in the kinematics data files);
- 1 at the bottom of the obstacle wall, farthest away from both tubes (referred to as *obsBot* in the kinematics data files);

The kinematic data are recorded at 150 Hz.

3.2 EMG

In the *dyad* experiment, 6 wireless Deslys Trigno EMG sensors are placed on each agent's right arm, on the following muscles:

- Flexor Carpi Ulnaris (FCU);
- Extensor Carpi Ulnaris (ECU);
- Biceps Brachii (BB);
- Triceps (Lateral Head) (TRI);
- Deltoid Anterior (DA);
- Deltoid Posterior (DP);

For the *solo* experiment, only 2 EMG sensors are used on the FCU and ECU muscles.

The EMG signal is recorded at 2 kHz. Then, the signal is filtered first through a 100ms window RMS, and then through a third order order low-pass Butterworth filter (fig. 6). For each participant, the maximum voluntary contraction (MVC) of each muscle is recorded prior to the experiment. The value of the EMG signal during the MVC is used in the post-processing step to normalize the EMG signal recorded during the task execution.

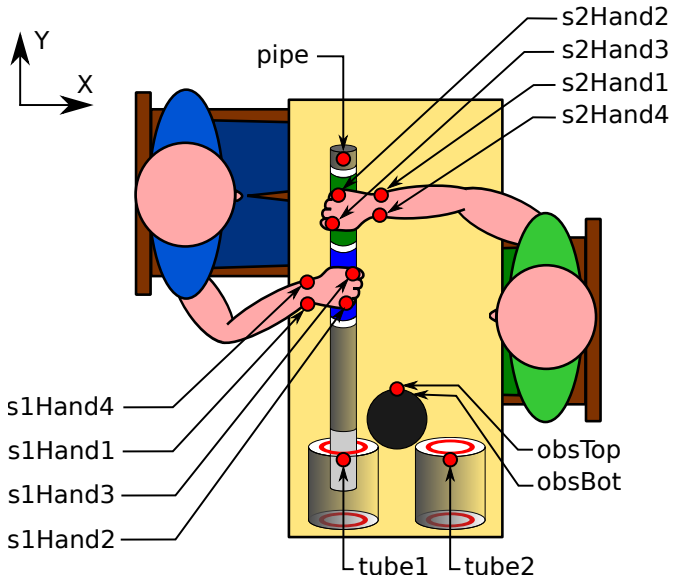

Figure 5: Positions of the Qualisys reflective markers: 4 markers are set on each agent's right hand, and 5 markers are set on the pipe, tubes and obstacle. Note that the *obsBottom* marker set on the obstacle is not visible, because it is vertically aligned with the *obsTop* marker.

3.2.1 Sensor Placement

The sensors are placed on the subject following guidance rules from the European project SENIAM [7], as well as location cues from Perroto, 2011 [6]. After we have located a muscle, the subject is asked to contract it to confirm the location of the "muscle belly", that is then marked with a pen. For each muscle, an EMG sensor is assigned, and annotated in our EMG acquisition software.

Before placing a sensor on a muscle location, the area surrounding the pen mark is prepared accordingly. The subject's skin is cleaned with alcohol until it acquires red tones, which indicates good skin impedance. After the alcohol dryes out, the EMG sensor is placed on the skin at the muscle fibers direction with the help of a double-sided sticker provided by the sensor manufacturer.

3.2.2 MVC measurement

For every muscle, the subject is asked to perform one isometric exercise [7] and the participants are instructed to contract each designated muscle for 3 s at their maximum capacity. We capture the maximum value from the EMG signal during the execution. The exercise, is performed 3 times, with a 1 minute interval between them to decrease fatigue effects. After the 3 trials, only the maximum value between them is stored as the respective muscle MVC by our acquisition software.

3.3 Performance

During the presentation of the task, participants are instructed to avoid contact between the pipe and the wall of the tubes. To detect such contacts, the end of the pipe is wrapped

(a) EMG signal processing steps: acquisition from sensor u_{raw}; RMS window of 100 ms (u_{rms}); Butterworth low pass third order filter with 10 Hz cutoff frequency(u_{fil}).

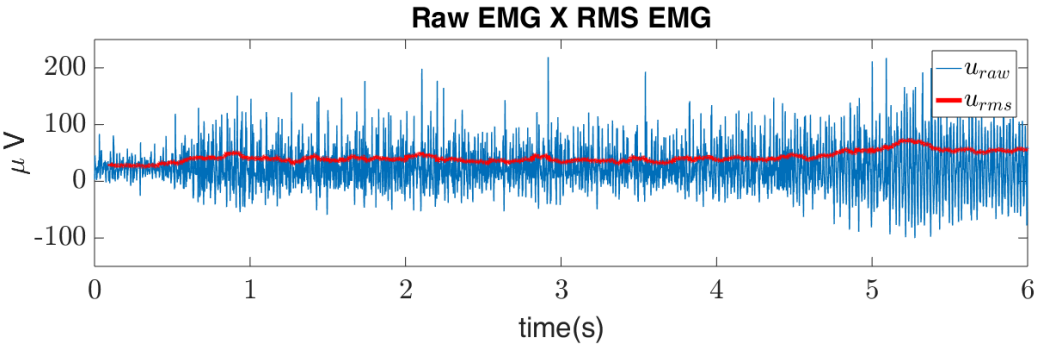

(b) Comparison between u_{raw}, and u_{rms}. It can be seen that u_{rms} is an envelope of u_{raw}.

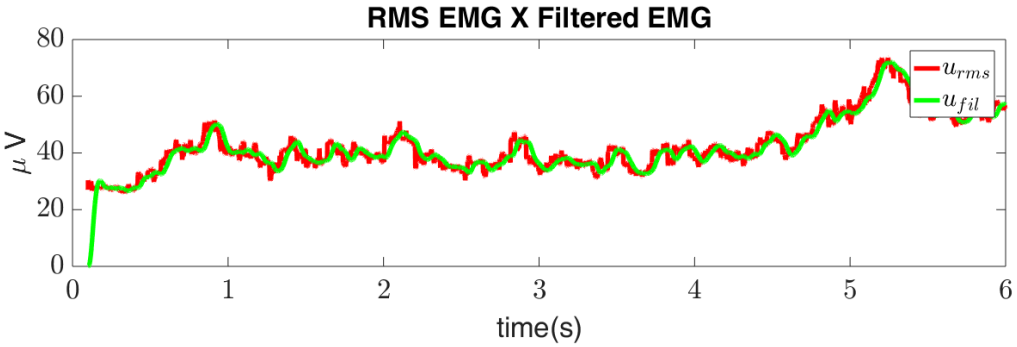

(c) Comparison between u_{rms}, and u_{fil}. The Butterworth filter smooths the RMS signal.

Figure 6: Steps to obtain an enveloped EMG signal for this work

Question Id	Question
1	Subject ID (Filled by Experimenter)
2	Age
3	Gender
4	Dominant Hand
5	How well do you feel today? (from 1, very tired, to 5, well rested)
6	Height (in cm)
7	Weight (in kg)
8	What is your current level of fitness? (1, None, to 5, Very sportive, fit)

Table 1: First part of the pre-experiment questionnaire

with aluminum foil, and metallic rings are placed inside the holes on the front and back walls of both tubes. A RaspberryPi is used to count the contacts on each ring.

The number of contacts between the pipe and the metallic rings on the front walls of the tubes is used as a performance measure. Only the onset of a contact is detected, so that whatever the duration of a contact, it counts as one contact only as long as it is maintained.

Given the reaction time of humans, and the fact that the aluminum foil is not perfectly flat, contacts that are separated by less that 0.5 s are counted as one single contact.

4 Pre-Experiment Questionnaire

Prior to any of the experiments, the subjects were submitted to a questionnaire (tables 1, and 2). The questions were split in 2 sections. The first part consisted of standard inquiries such as gender, dominant hand, height or weight. And in the second part, we inquired the subjects for their desirability of control (DC), according to a known psychology scale [1].

The authors of the desirability of control scale stated that their test was designed to measure individual differences in the general desire for control over the events in their lives. Moreover, They make the case that people with high levels in the DC scale can be described as assertive, actively seeking to avoid failures and ensure desired outcomes by controlling events on their reach.

5 Data files

The raw data for EMG signal, motion measurements, and number of wall touches is freely available in Zenodo at the DOI: 10.5281/zenodo.3989616 [3]. For each experiment EXP (*single* or *dyad*) there are 5 folders containing the data files:

- **EXP-qualisys-data:** Contains the Qualisys .qtm files of all recorded trials. For the dyad experiment, each file is named "Dyad_X_Cond_Y_Trial_Z.qtm" where X is the dyad number, Y one of the 3 conditions described in section 2.1 ("0L" for natural behaviour, "1L" for Participant 1 Leader, "2L" for Participant 2 Leader), and Z the number of the trials. For the "single" experiment, the files are named

Please read each statement carefully and respond to it by expressing the extent to which you believe the statement applies to you.
For all items, a response from 1 to 7 is required. Use the number that best reflects your belief when the scale is defined as follows:
1 = The statement does not apply to me at all
2 = The statement usually does not apply to me
3 = Most often, the statement does not apply
4 = I am unsure about whether or not the statement applies to me, or it applies to me about half the time
5 = The statement applies more often than not
6 = The statement usually applies to me
7 = The statement always applies to me

Question Id	Question
9	I have a job where I have a lot of control over what I do and when I do it.
10	I enjoy political participation because I want to have as much of a say in running government as possible.
11	I try to avoid situations where someone else tells me what to do.
12	I would prefer to be a leader than a follower
13	I enjoy being able to influence the actions of others
14	I am careful to check everything on an automobile before I leave for a long trip
15	Others usually know what is best for me
16	I enjoy making my own decisions
17	I enjoy having control over my own destiny
18	I would rather someone else take over the leadership role when I am involved in a group project.
19	I consider myself to be generally more capable of handling situations than others are
20	I would rather run my own business and make my own mistakes than listen to someone else's orders.
21	I like to get a good idea of what a job is about before I begin.
22	When I see a problem, I prefer to do something about it rather than sit by and let it continue.
23	When it comes to orders, I would rather give them than receive them.
24	I wish I could push many of life's daily decisions off on someone else.
25	When driving, I try to avoid putting myself in a situation where I could be hurt by another person's mistake.
26	I prefer to avoid situations where someone else has to tell me what it is I should be doing.
27	There are many situation in which I would prefer only one choide rather than having to make a decision.
28	I like to wait and see if someone else is going to solve a problem so that I do not have to be bothered with it.

Table 2: Second part of the pre-experiment questionnaire: The desire for control scale [1]

"Single_X_Cond_Y_Trial_Z.csv" where X is the participant number, Y one of the 2 conditions ("S1" when the participant seats as Participant 1, "S2" when the participant seats as Participant 2), and Z the number of the trial. Note that trials are numbered from 1 to 15 so that the order in which the 3 conditions were performed for this specific dyad can easily be retrieved (1 to 5 being the first condition, 6 to 10 the second condition, and 11 to 15 the third condition).

- **EXP-kinematic-data:** Contains the motion capture data of all recorded trials in .csv files. Each file is named "Dyad_X_Cond_Y_Trial_Z_Kinematic.csv" (in the *single* experiment "Dyad" is replaced by "Single"). The motion capture data are the trajectories of the 3D Cartesian position (X, Y, Z with Y parallel to the tubes axis and Z up) of the Qualisys markers set on the participants' right arm and on the pipe, tubes and obstacle. Units are *mm*. When a marker is lost for a duration too long to interpolate reliably, the corresponding X, Y, Z values of the corresponding time frames are empty.

- **EXP-EMG-data:** Contains the EMG signal of each of the EMG sensors placed of each of the participants' right arm (12 sensors in total) in .csv files. Each file is named "Dyad_X_Cond_Y_Trial_Z_EMG.csv" (in the *single* experiment "Dyad" is replaced by "Single"). Units are μV. Each EMG channel is designated by its Delsys number (can be between 1 and 16). The matching between the EMG channels and the participants' muscles is given in the configuration file. Note that the data from the Qualisys and from the EMG are synchronized because they were all recorded using the Qualisys software (recording of Delsys EMG signal is embedded in the Qualisys software).

- **EXP-performance-measure-walltouches:** Contains the pipe/tubes front walls contact signals of all recorded trials. Each file is named "Dyad_X_Cond_Y_Trial_Z_Performance.csv" (in the *single* experiment "Dyad" is replaced by "Single"). The columns *input1*, *input2*, *input3*, *input4* correspond to contacts between the pipe and the following walls of the tubes:

  - *input1:* back wall of Tube 1;
  - *input2:* front wall of Tube 1;
  - *input3:* front wall of Tube 2;
  - *input4:* back wall of Tube 2;

  A 1 indicates that a contact is detected for the corresponding input, at the time indicated in the first column. Each file should contain at least 2 lines of data: one contact on *input1* to indicate the beginning of the task and one contact with *input4* to indicate the end of the task. However, the start or end signals (*i.e.* these two lines) are missing in a small number of files because the participants did not make contact when starting/finishing the movement. Note that the contact detection is not synchronized with the Qualisys and EMG, so the timing of the contacts cannot be directly compared with the timing of the motion capture and EMG data.

- **EXP-MVC-calibration:** Each dyad contains 2 .csv files with the values of the EMG signal during the Maximum Voluntary Contraction (MVC) measurement. The 2 files correspond to each of the 2 participants in the dyad, and are named "ID_X_Pos_Y_Calibration .csv" where X is the participant ID, Y the position of the participant ("S1" for Participant 1, "S2" for Participant 2). Each file contains a line with first the EMG sensor ID, followed by the value of the signal during the MVC. Units are V. For the *dyad* experiment, the 6 EMG sensors are given in the following order: Flexor carpi ulnaris, Extensor carpi ulnaris, Biceps Brachii, Triceps Lateral Head, Deltoid, Anterior, Deltoid, Posterior. For the *single* experiment, "Pos_Y" disappears in the filename, and there are only 2 EMG sensors in the following order: Flexor carpi ulnaris, Extensor carpi ulnaris. For each muscle, the MVC is the maximum value of the EMG signal obtained during a "burst" force static contraction of 3 s, repeated 3 times with 60 s of rest between each contraction.

In addition, the dataset contains two Excel configuration files "**Configuration_Dyad .xls**" and "**Configuration_Single.xls**". These files contain the date and time at which the experiment was performed for each dyad/single, the dyad/single number, the participant(s) ID (used to anonymize the data), the seat position of each participant (in the *dyad* experiment only), the order in which the different conditions were performed, the matching between the EMG sensors ID and the muscles, lengths of the participants' arm segments, and information relative to physical condition of the participants. The upper arm length is measured from the Acromion to the Lateral Epicondyle. The forearm length is measured from the Lateral Epicondyle to the Ulna Styloid Process. The hand length is measured from the Ulna Styloid Process to the Head of the 5th Metacarpal, while the hand is aligned with the forearm.

6 Methods for Data Analysis

6.1 Timing Measurements

There are 3 important timing measurements for this experiment (fig. 7): $t_{EXIT}, t_{MID}, t_{ENT}$. They are the instants in which the pipe exits tube 1, in which the pipe goes around the obstacle, and in which the pipe enters tube 2. In order to obtain those instants, first, we calculate the centroid of hand markers of both participants $\vec{r} = (r_x, r_y)$. And then we obtain

$$t_{EXIT} = t(|r_y - tube_{1y}| < 0.35) \tag{1}$$

where $tube_{1X}$ is the Y component of the tube 1 position, and 0.35 is the distance from the middle of the handles to the end of the tube (fig. 2). The same is done for t_{ENTER}:

$$t_{ENTER} = t(|r_y - tube_{2y}| < 0.35) \tag{2}$$

And finally, t_{MIDDLE} is the instant after t_{EXIT} and before t_{ENTER} in which r_y starts decreasing instead of increasing. The files are in the "/PostProcessed_Data .../Timing/" folder in the format "Dyad_X_Timing.txt".

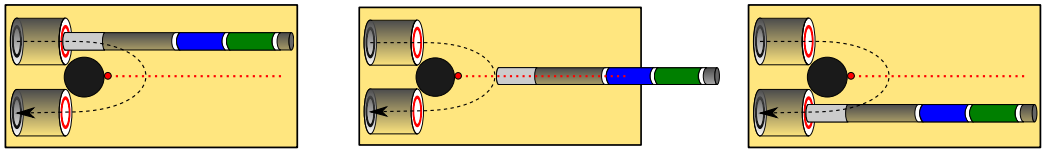

(a) $t = t_{EXIT}$ (b) $t = t_{MID}$ (c) $t = t_{ENT}$

Figure 7: Sequence of key instants during the manipulation

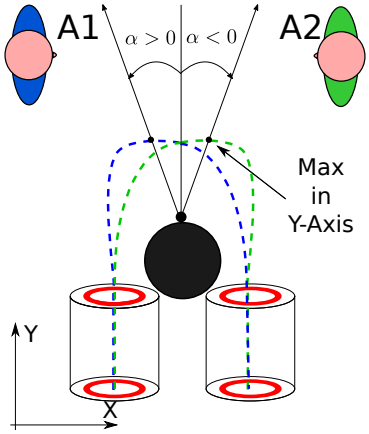

Figure 8: Angle of trajectory deviation, α: It is the angle between the vertical line that divides the setup symmetrically, and the line from the obstacle marker to the point of the trajectory with maximum value in the Y-Axis

6.2 Index of Co-Contraction

A way for indirectly quantifying human joint stiffness is to compare the levels of activation/contraction (obtained from normalized EMG signals acquired from maximum values of contraction in a calibration phase prior to the experiment) from a pair of antagonist muscles, and then use the minimum value of both. This can be summarized by an index of co-contraction (ICC) as used in [4, 5, 8]:

$$icc_k(t) = min(u^i_{norm}(t), u^j_{norm}(t)) \tag{3}$$

where the normalized EMG signal is given by u_{norm}, and the ICC of a joint k whose antagonist muscles are i and j is given by icc_k. It is also worth mentioning that the ICC is only directly proportional to the joint stiffness. Therefore, whenever a joint is more or less stiff the ICC related to the joint will increase or decrease.

The files are in the format "Dyad_X_Cond_Y_Trial_Z_ICC.csv".

6.3 Deviation Angle

The deviation angle, α, measures the skewness of the trajectory with respect to the Y-axis that divides the experimental setup symmetrically. Given the trajectory hand markers centroid $\vec{r}(t)$ trajectory we calculate the point in which the position is maximum in the Y-axis

$$t_{max} = \arg\max(r_y) \tag{4}$$

$$\vec{r}_{max} = \vec{r}(t_{max}) \tag{5}$$

and the position of the marker in front of the obstacle $\vec{r}_{obs}$ to be able to calculate a vector that indicates the direction of the skew

$$\vec{r}_{dir} = \vec{r}_{max} - \vec{r}_{obs} \tag{6}$$

Finally, the angle α is defined as the minimum angle between the Y-Axis vector and $\vec{r}_{dir}$. The data files are in the folder "PostProcessed_Data_/Deviation_Angles/" in one solo file "Deviation_Angles_Dyad_txt"

6.4 Statistical Analysis Methods

6.4.1 Contact Sensor Data

The data from the contact sensors is made of integer values, and always positive, therefore, the sample is not Gaussian, it is in fact classified as count data. After verifying that the count data was overdispersed (variances larger than means) in both experiments, we used a general linear mixed model, with random effects to account for the repetitions in the same condition, along with negative binomial distributions [2]. Since there are 3 conditions, post hoc tests with Tukey correction were used to evaluate if the different conditions affected the number of contacts.

6.4.2 Index of Co-Contraction Data

For each executed trial, a time series of indexes of co-contraction is calculated (eq. 3). In order to have a unique measure of stiffness throughout the entire task we calculated the root mean square (icc_{rms}) of every time series. Then, we used Shapiro tests to verify if the (icc_{rms}) had a normal distribution regarding the position. For participants 1 and 2 the Shapiro test revealed that the (icc_{rms}) was not normally distributed ($p < 0.001$). So, we used Friedman tests instead of regular ANOVA. To do that, we grouped the 5 ICC measurements from each condition and each participant into one median value.

6.4.3 Deviation Angle Data

The deviation angle from experiments was verified to have a normal distribution for both experiments using the Shapiro-Wilk normality test (Dyad manipulation: p = .39; Solo Manipulation: p = .05), therefore, a regular analysis of variance with repeated measures (or a paired t-test for the solo experiment) was done to verify the effect of the conditions on the deviation angle.

7 Result Figures

7.1 Index of Co-Contraction

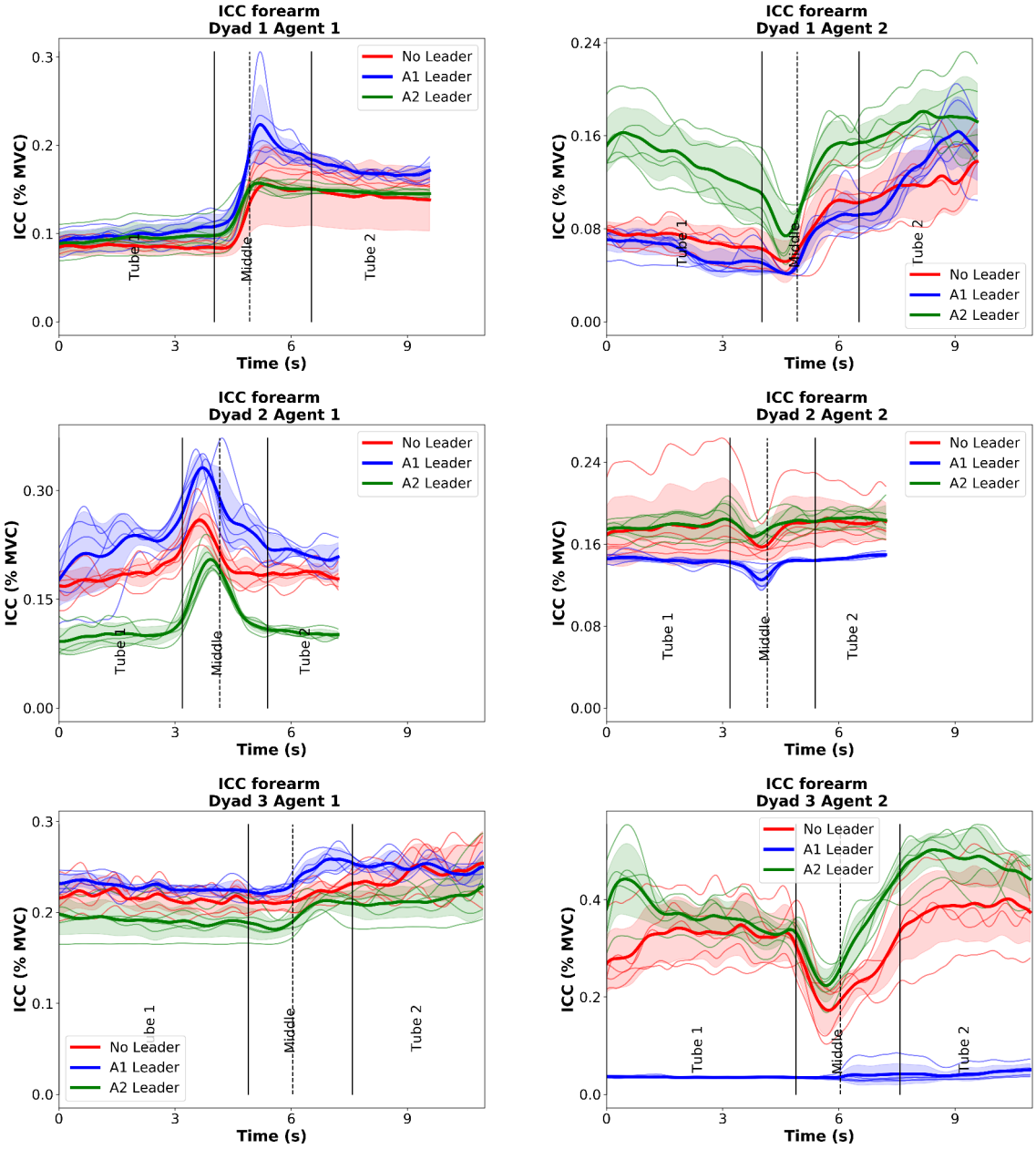

Figure 9: Average Index of Co-Contraction for dyads 1,2 and 3 for all conditions on the Dyad Experiment

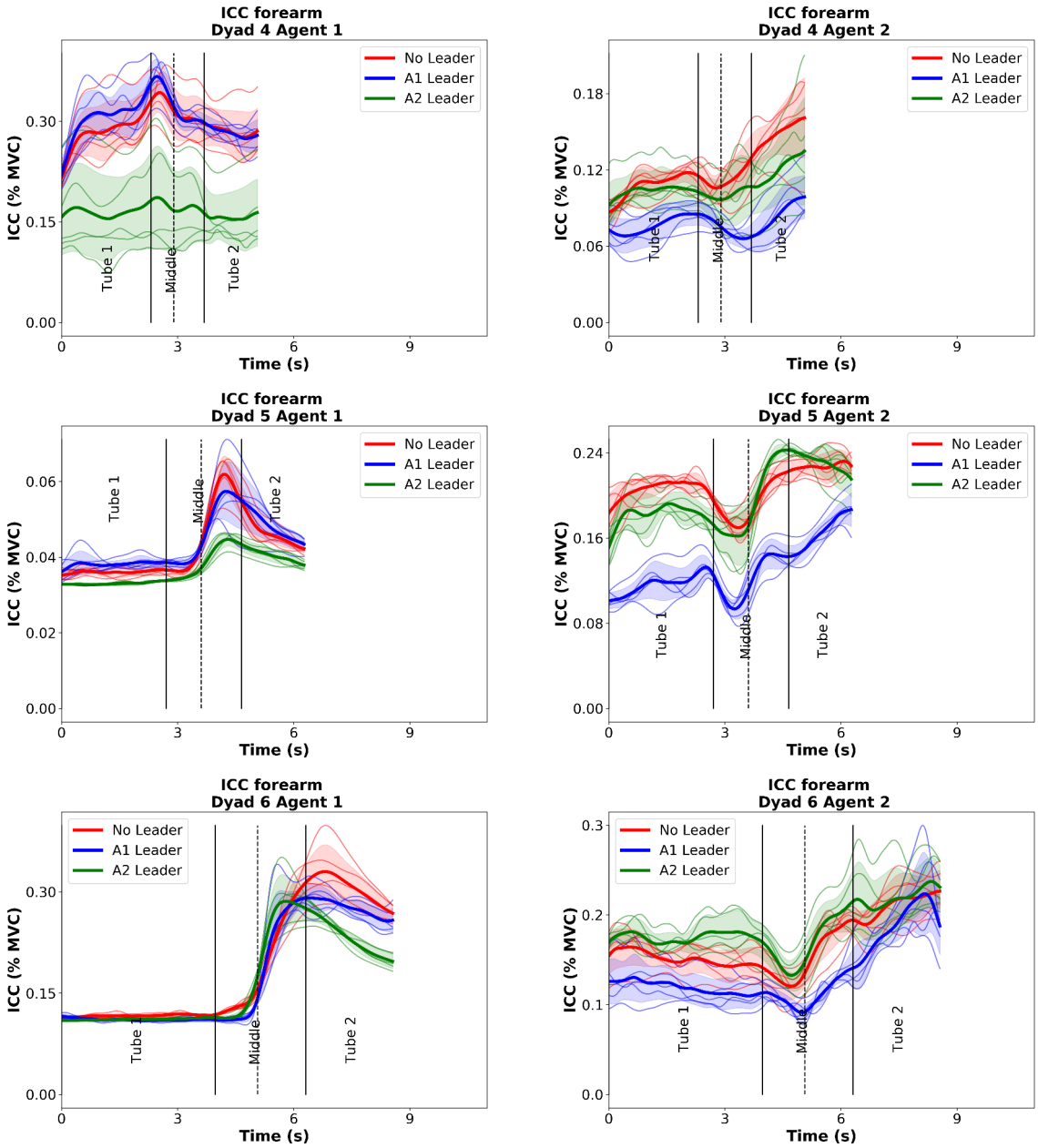

Figure 10: Average Index of Co-Contraction for dyads 4,5 and 6 for all conditions on the Dyad Experiment

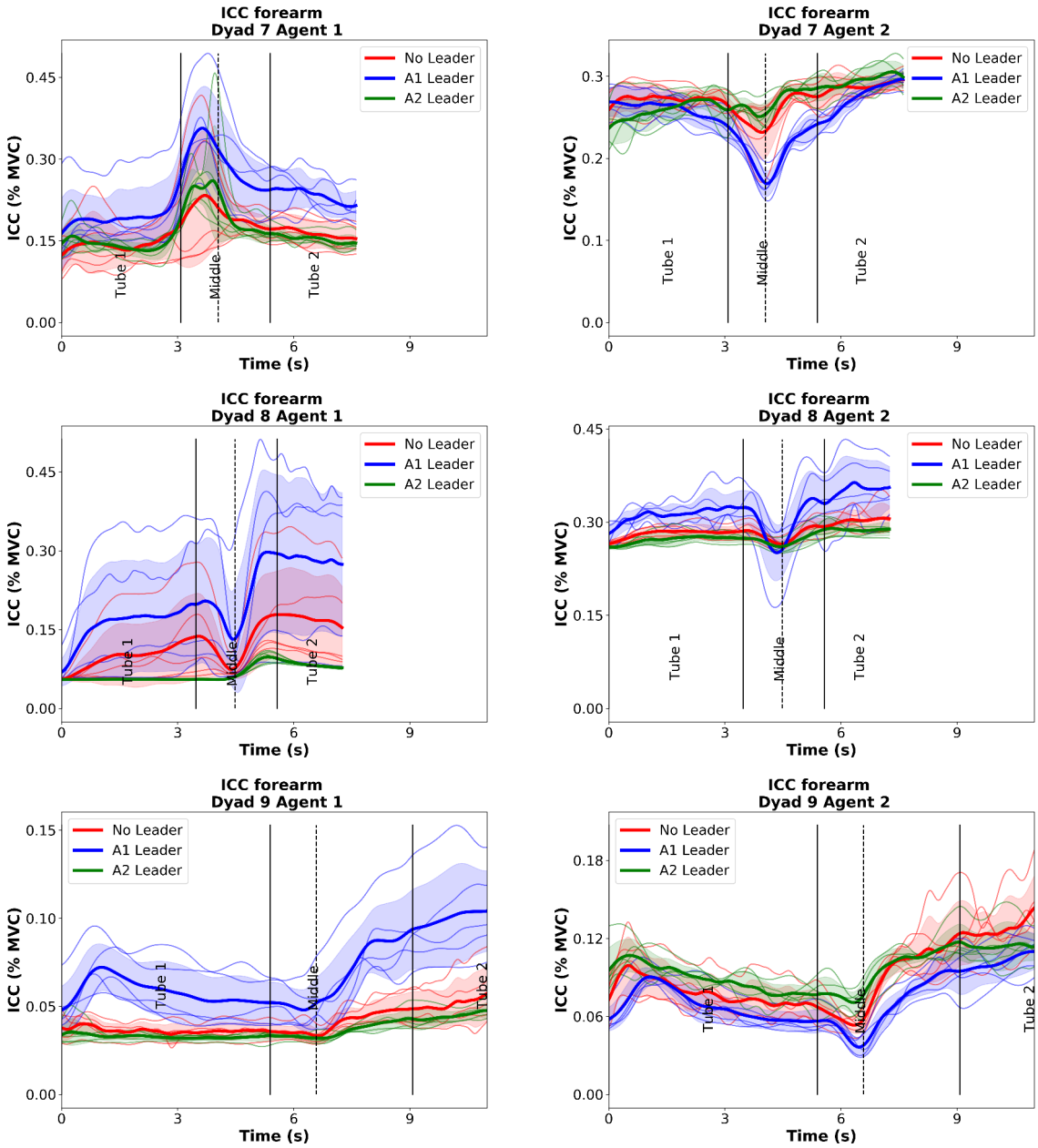

Figure 11: Average Index of Co-Contraction for dyads 7,8 and 9 for all conditions on the Dyad Experiment

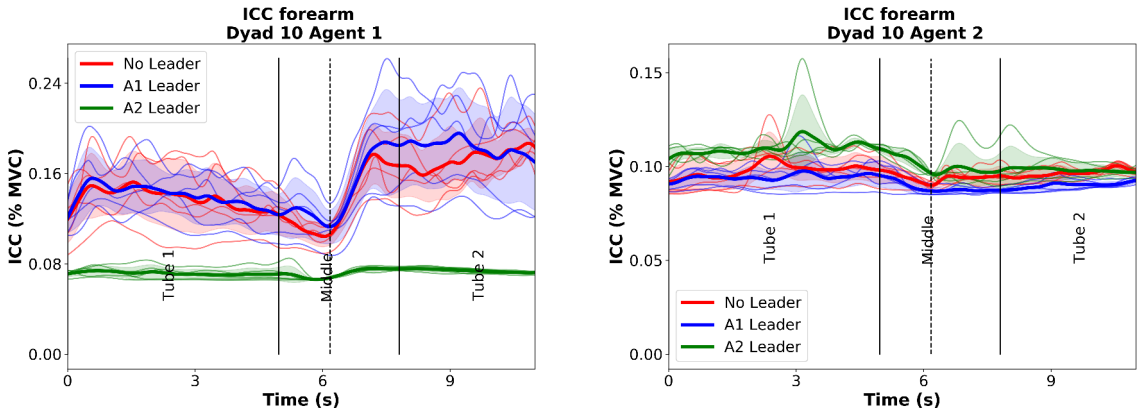

Figure 12: Average Index of Co-Contraction for dyads 10 for all conditions on the Dyad Experiment

7.2 Pipe Trajectory

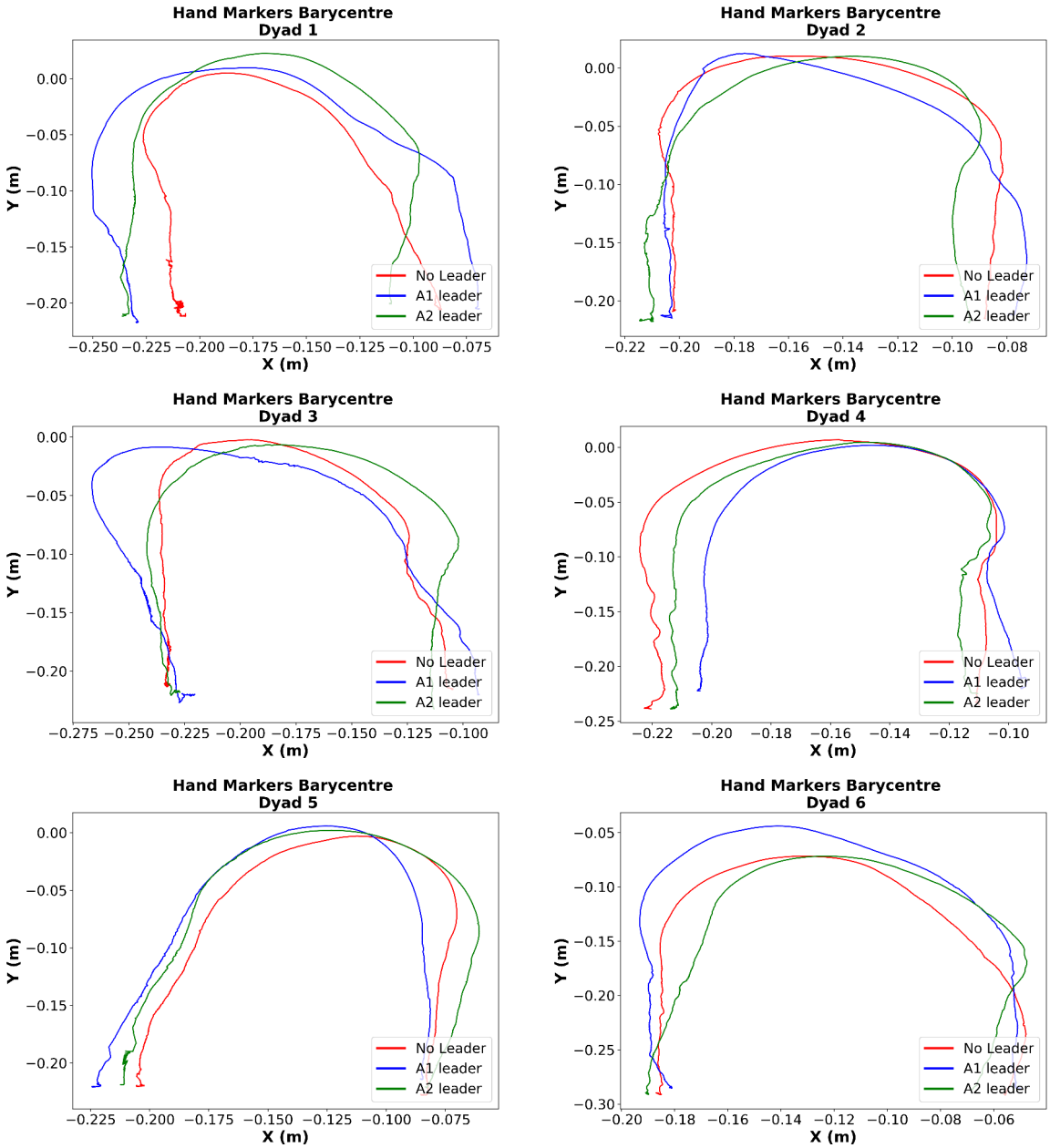

Figure 13: Trajectory of the barycentre of the agents' hands as a proxy to the center of the pipe. Dyads 1 to 6

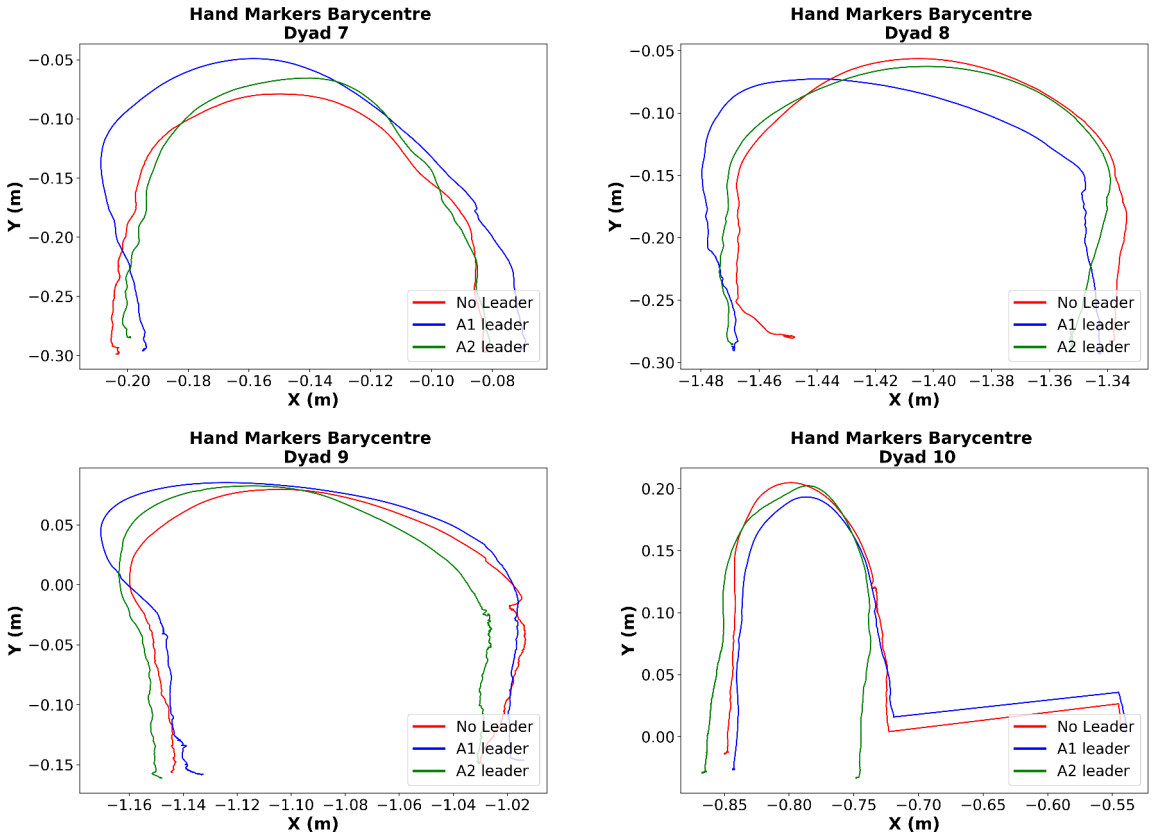

Figure 14: Trajectory of the barycentre of the agents' hands as a proxy to the center of the pipe. Dyads 7 to 10

References

[1] Jerry M Burger and Harris M Cooper. The desirability of control. *Motivation and emotion*, 3(4):381–393, 1979.

[2] A. Colin Cameron and Pravin K. Trivedi. *Regression Analysis of Count Data*. Econometric Society Monographs. Cambridge University Press, 2 edition, 2013.

[3] Waldez Gomes, Pauline Maurice, and Serena Ivaldi. Andy data - human human object co-manipulation, August 2020. Dataset available at https://doi.org/10.5281/zenodo.3989616.

[4] S. Grafakos, F. Dimeas, and N. Aspragathos. Variable admittance control in phri using emg-based arm muscles co-activation. In *2016 IEEE International Conference on Systems, Man, and Cybernetics (SMC)*, pages 001900–001905, Oct 2016.

[5] Paul L. Gribble, Lucy I. Mullin, Nicholas Cothros, and Andrew Mattar. Role of cocontraction in arm movement accuracy. *Journal of Neurophysiology*, 89(5):2396–2405, 2003.

[6] Aldo O Perotto. *Anatomical guide for the electromyographer: the limbs and trunk*. Charles C Thomas Publisher, 2011.

[7] D Stegeman and H Hermens. Standards for surface electromyography: The european project surface emg for non-invasive assessment of muscles (seniam). 2007.

[8] Kurt A. Thoroughman and Reza Shadmehr. Electromyographic correlates of learning an internal model of reaching movements. *Journal of Neuroscience*, 19(19):8573–8588, 1999.